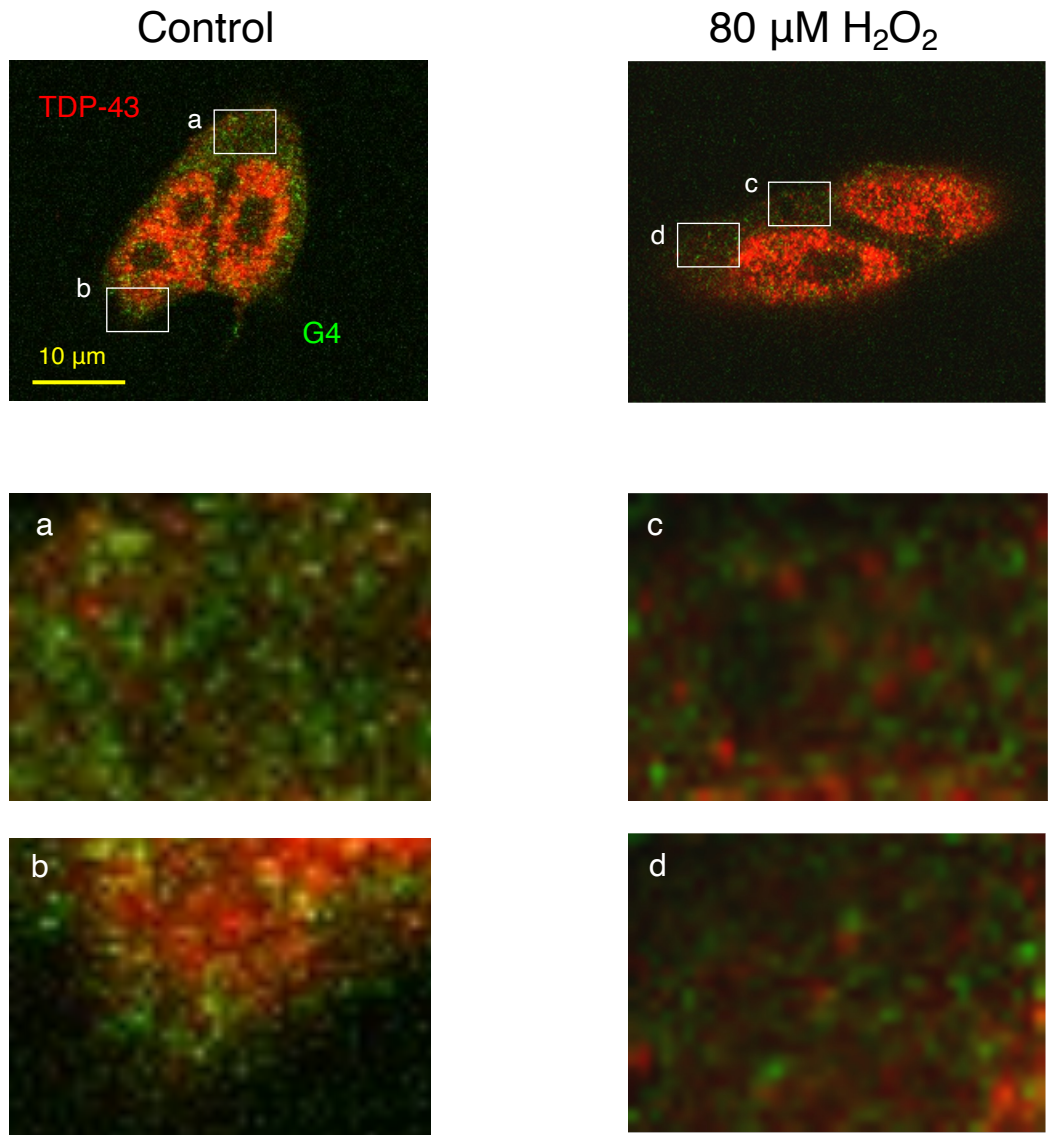


**Table S1.** Synthesized oligonucleotides used in this study.

(Uppercase letters indicate RNA, lowercase letters indicate DNA)

Name	Sequences (5' to 3') [modification]	Length
PSD-95-G4	GGGGAAAAGGGAGGGAUAGGG	20
A <sub>x647</sub> PSD95-G4	[Alexa Fluor 647]-GGGGAAAAGGGAGGGAUAGGG	20
PSD-95-G4 (10 % 8OG)	aaaaaAAAAAaaaaAaaaaAUaaa	20
PSD-95-G4 (20 % 8OG)	ββββAAAAβββAβββAUβββ	20
PSD-95-G4 (40 % 8OG)	YYYYAAAAYYYAYYYAUYYY	20
CaMKIIa-G4	UGGGGGGGGGCGGGUGGGGA	18
A <sub>x647</sub> CaMKIIa-G4	[Alexa Fluor 647]-UGGGGGGGGGCGGGUGGGGA	18
CaMKIIa-G4 (10 % 8OG)	UaaaaaaaCaaaaUaaaaA	18
CaMKIIa-G4 (20 % 8OG)	UβββββββCβββUβββA	18
CaMKIIa-G4 (40 % 8OG)	UYYYYYYYYYCYYYYUYYYYA	18
C9ORF72 HRE <sub>4</sub>	ggggccggggccggggccggggcc	24
Teromere <sub>4</sub>	gggttagggtttagggtttagggttta	24
cMyc	ggggagggtggggagggtgggggt	23
UG <sub>12</sub>	UGUGUGUGUGUGUGUGUGUGUGUGUG	24
G <sub>3</sub> UG <sub>3</sub>	GGGUGGG	7

$\alpha$  = 8-oxoguanine (10 %); RNA G (90 %)  
 $\beta$  = 8-oxoguanine (20 %); RNA G (80 %)  
 $\gamma$  = 8-oxoguanine (40 %); RNA G (60 %)



**Figure S1.** High-magnification image showing the localization of TPD-43 and G4 (related to Fig. 1B).

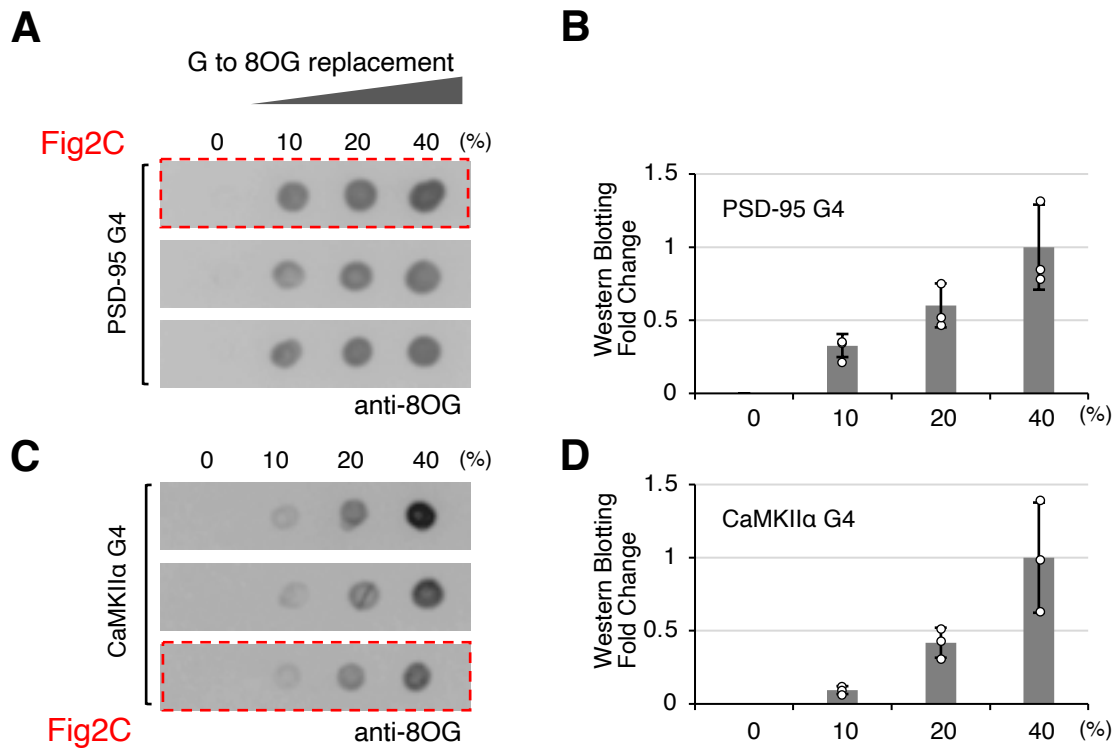


**Figure S2.** Dot–blot Western blotting of 8OG-modified RNAs. **(A, C)** The nonoxidized and oxidized forms of three types of RNAs (2.5 pmol each) derived from PSD-95-G4 and CaMKII $\alpha$ -G4 were spotted onto a nylon membrane and analyzed by Western blotting. The regions outlined by the red dashed lines were used for quantification in Fig. 2C. **(B, D)** Experiments were performed in triplicate, and the data are presented as the mean  $\pm$  SEM.

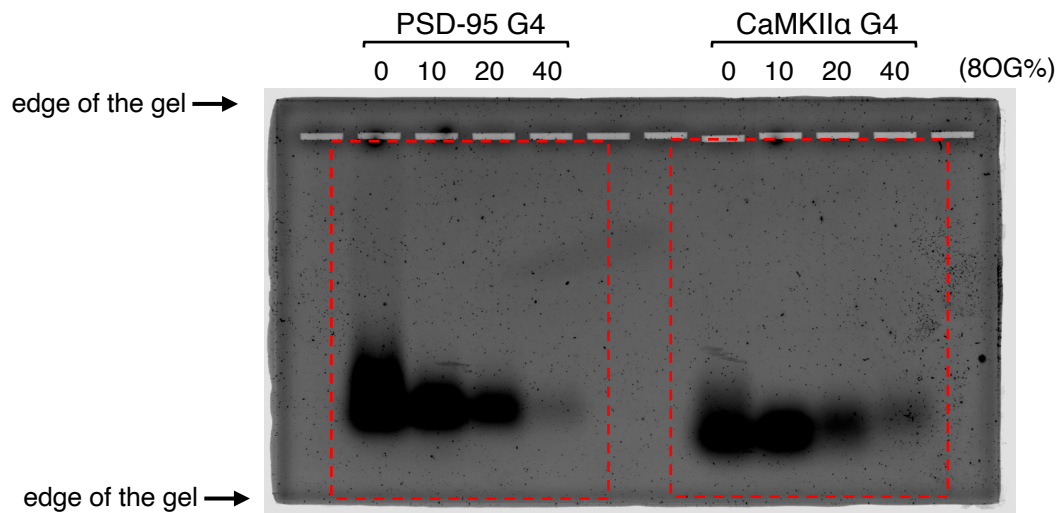
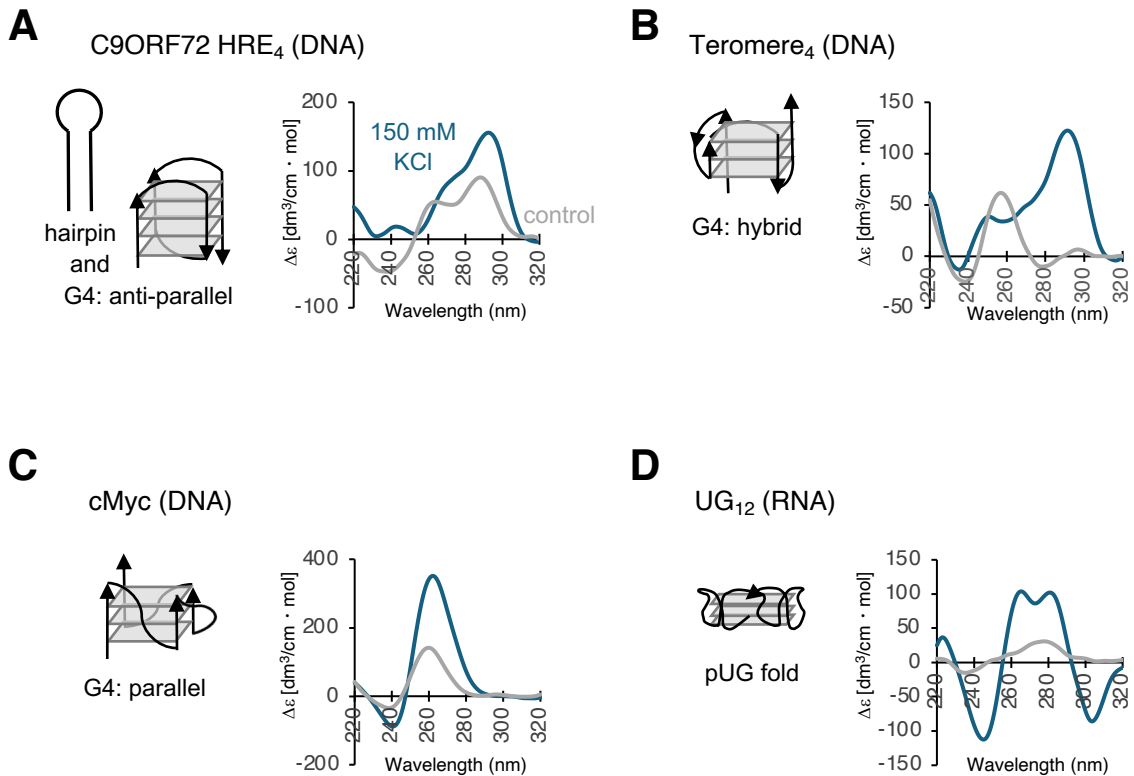
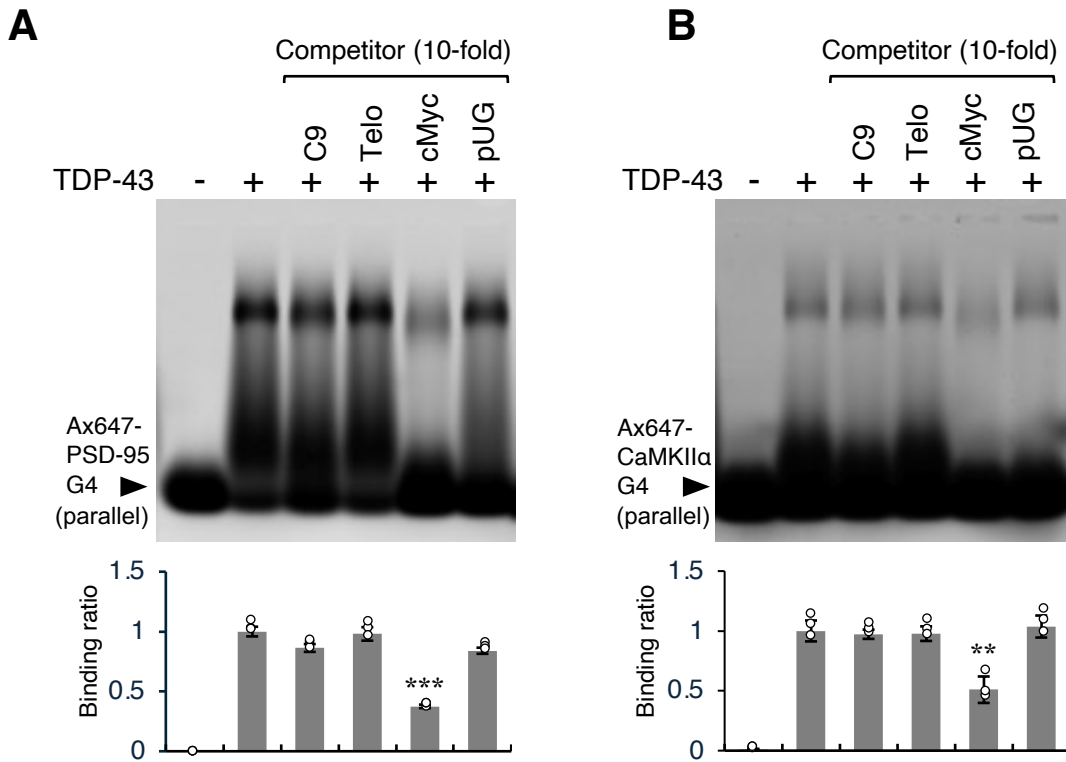


Fig2D

**Figure S3.** Agarose gel electrophoresis (related to Fig. 2D). The nonoxidized and oxidized forms of the three types of RNAs (25 pmol each) derived from PSD-95-G4 and CaMKIIa-G4 were electrophoresed on a 1% agarose gel containing  $0.5 \times$  TBE under native conditions. The gel was stained with the intercalating fluorescent dye SYBR Green II. The regions outlined by the red dashed lines were used for Fig. 2D.



**Figure S4.** CD spectra of four different conformations. The predicted structures of the synthesized DNA/RNAs were confirmed by CD spectral analysis using 2  $\mu$ M oligonucleotides in the presence or absence (control) of 150 mM KCl. The measurements were repeated five times, and the average spectra are shown. **(A)** CD spectrum of C9ORF72 HRE<sub>4</sub> DNA (a mixture of hairpin and antiparallel G4 structures). **(B)** CD spectra of Teromere<sub>4</sub> DNA (hybrid G4). **(C)** CD spectra of cMyc DNA (parallel G4). **(D)** CD spectra of UG<sub>12</sub> fold (pUG fold). Traces are shown in the presence and absence of 150 mM KCl.



**Figure S5.** Binding specificity of TDP-43. 0.5 pmol of fluorescently labeled G4 probe (**A**; Ax647-PSD-95-G4 or **B**; Ax647-CaMKII $\alpha$ -G4) was mixed with TDP-43 (2 pmol) and the indicated unlabeled competitors (10-fold for probe) and electrophoresed under nondenaturing conditions. Each overshifted band was quantified, and the mean and standard error ( $\pm$  SEM) were calculated from three independent experiments. The results are shown in the graph, with the y-axis representing the mean  $\pm$  SEM. Statistical significance was assessed using a two-tailed Student's *t*-test. \*\**P* < 0.01, \*\*\**P* < 0.001.

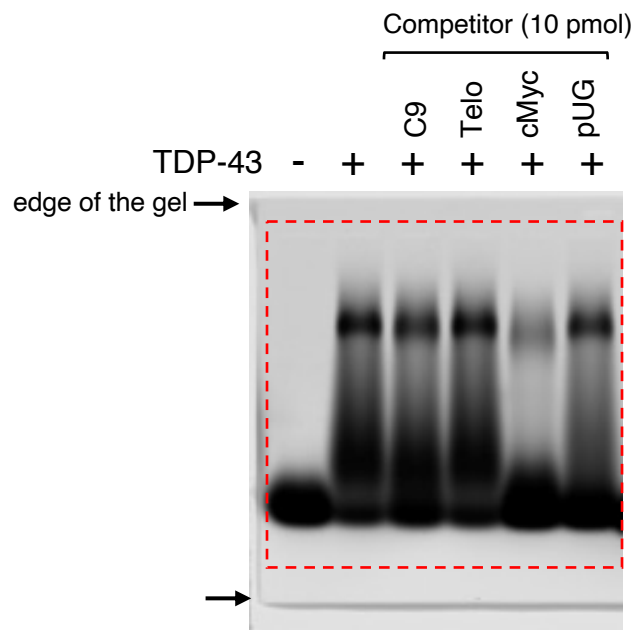
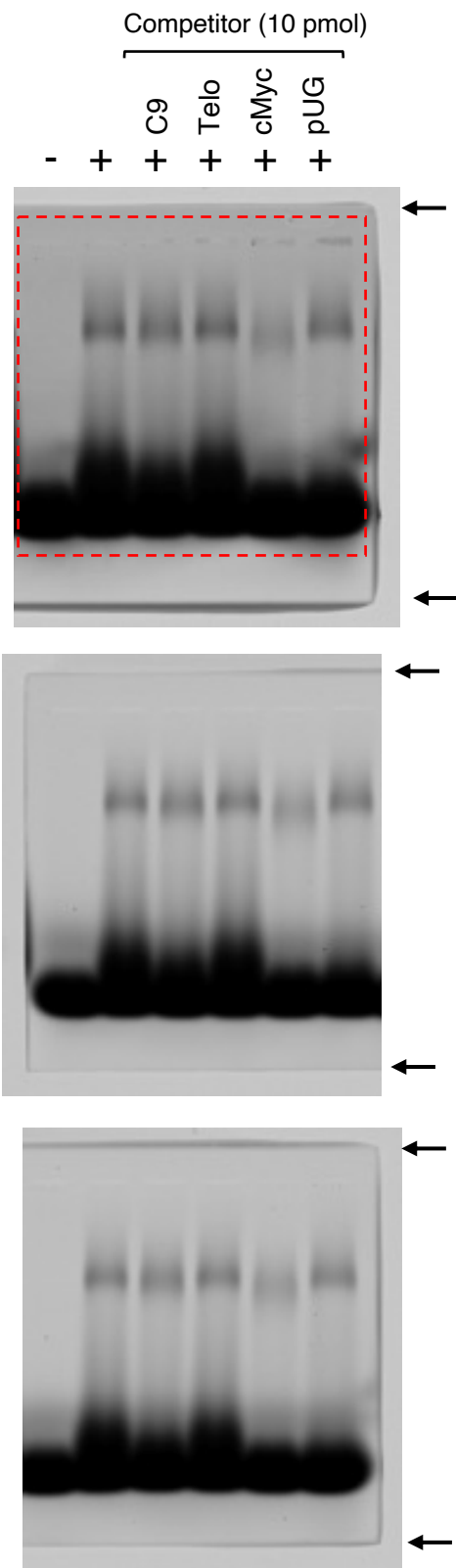


Fig. S5

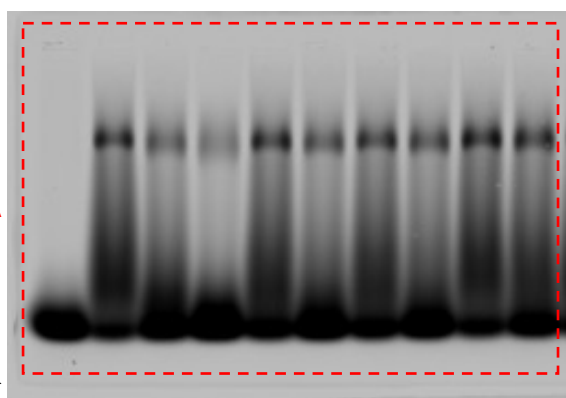


**Figure S6.** Original images of the gel shift assay (related to Fig. S5). The areas enclosed by the red dashed lines are used for Fig. S5.

PSD-95 G4		8OG								
		0 %		10 %		20 %		40 %		
Comp	-	-	3	10	3	10	3	10	3	10
TDP-43	-	+	+	+	+	+	+	+	+	+

→  
edge  
of the  
gel

Fig. 4A



CaMKII $\alpha$ G4		8OG								
		0 %		10 %		20 %		40 %		
-	-	-	3	10	3	10	3	10	3	10
-	+	+	+	+	+	+	+	+	+	+

→

Fig. 4B

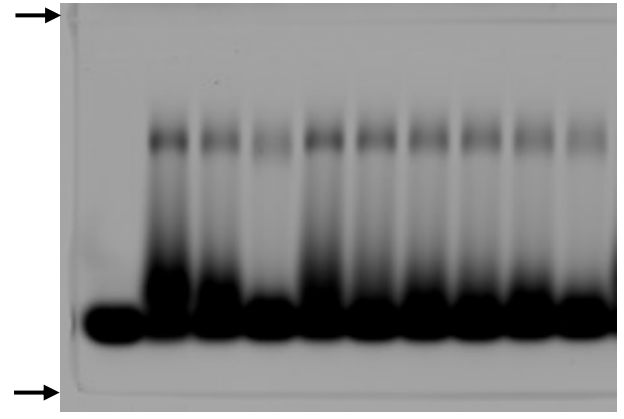
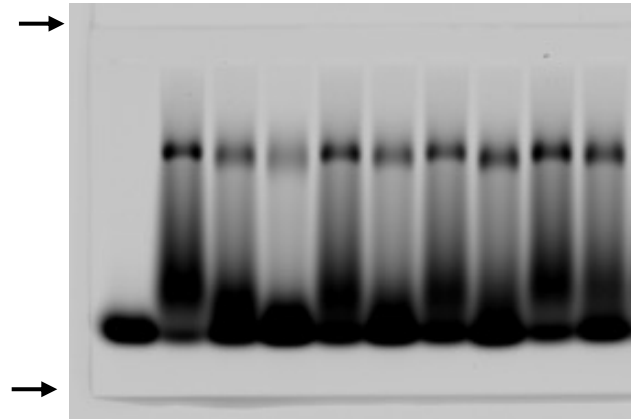
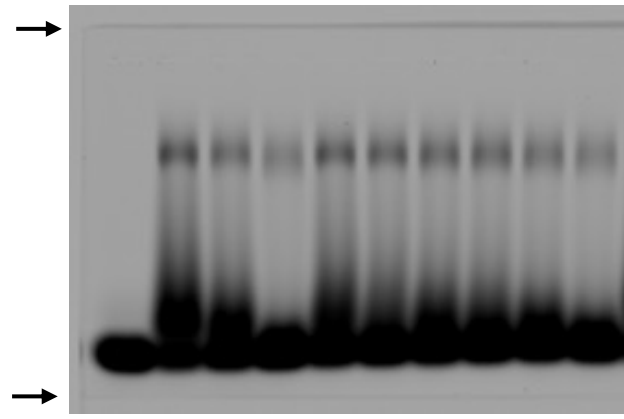
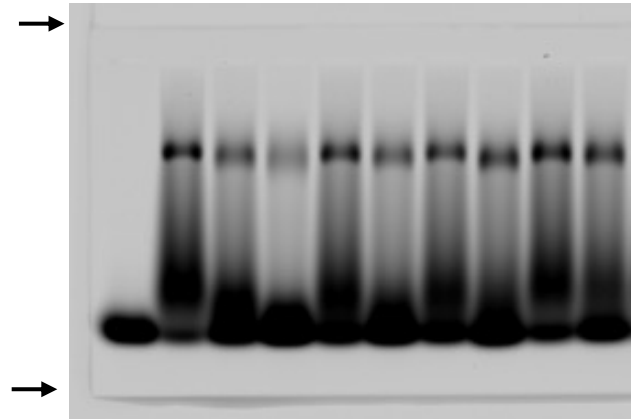
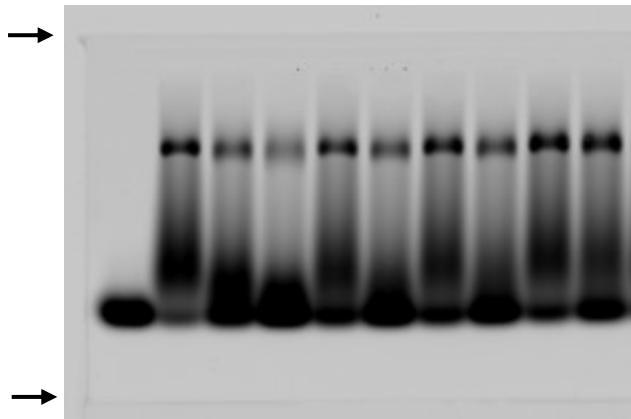
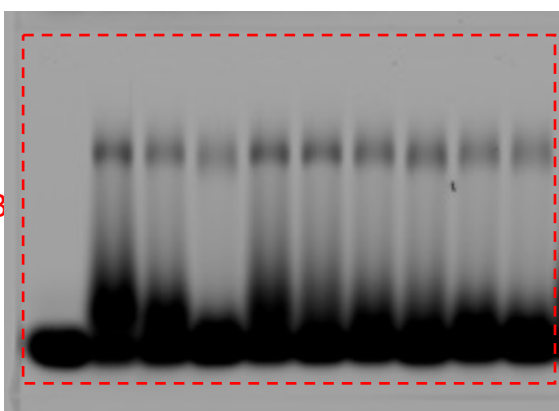


**Figure S7.** Original images of the gel shift assay (related to Fig. 4). The areas enclosed by the red dashed lines are used for Fig. 4A and B.

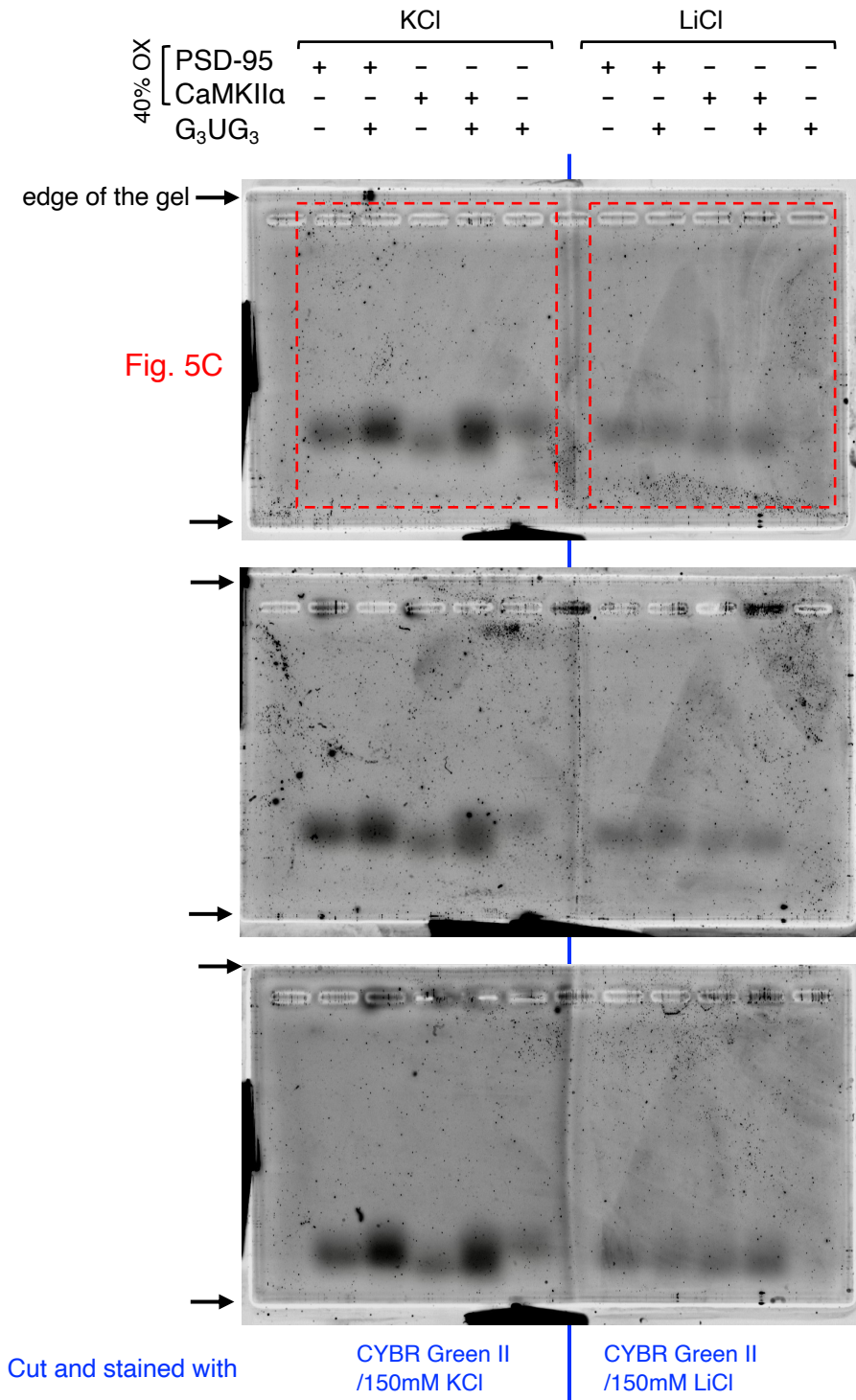


**Figure S8.** Original images of electrophoresis (related to Fig. 5C). The areas enclosed by the red dashed lines are used for Fig. 5C. The samples containing potassium or lithium were electrophoresed simultaneously on the same gel, cut upon completion, and stained with a CYBR Green II staining solution containing 150 mM KCl or LiCl.

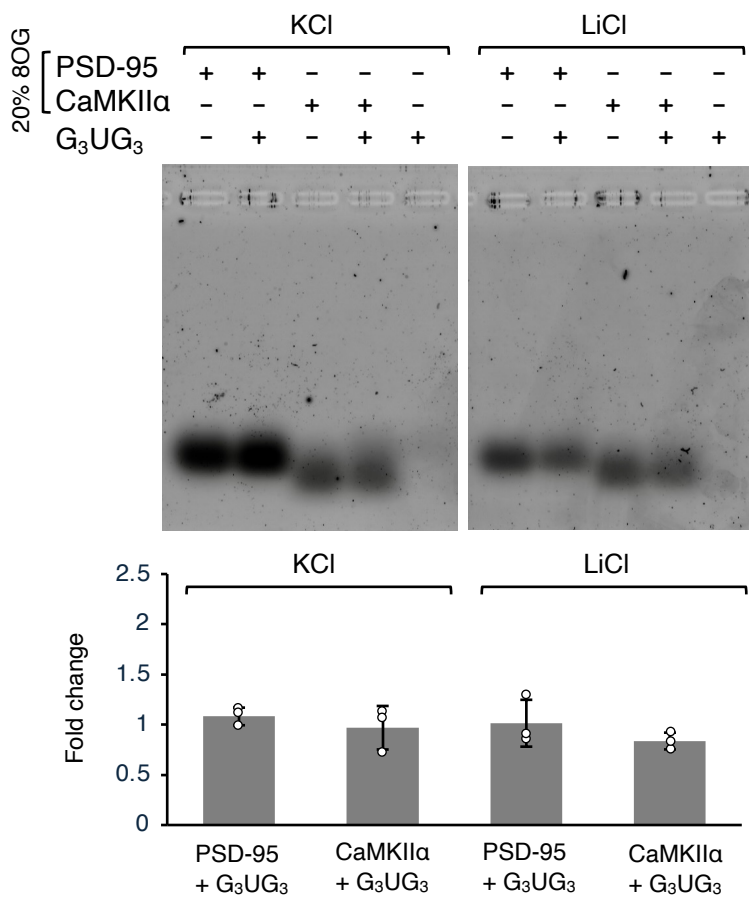


**Figure S9.** G4 formation assay. The indicated 20% oxidized RNAs (20 pmol) were mixed with the absence or presence of  $G_3UG_3$  (20 pmol) and electrophoresed on 1% agarose gel under native conditions. The gels were stained with the intercalating fluorescent dye SYBR Green II, and the individual signals were quantified. The graph below shows the fold change after the addition of  $G_3UG_3$ , which was calculated by subtracting the signal for  $G_3UG_3$  alone from the value for mixing 20% oxidized PSD-95 or CaMKII $\alpha$  RNAs with  $G_3UG_3$ . The experiments were performed in triplicate, and the data are presented as the mean  $\pm$  SEM.

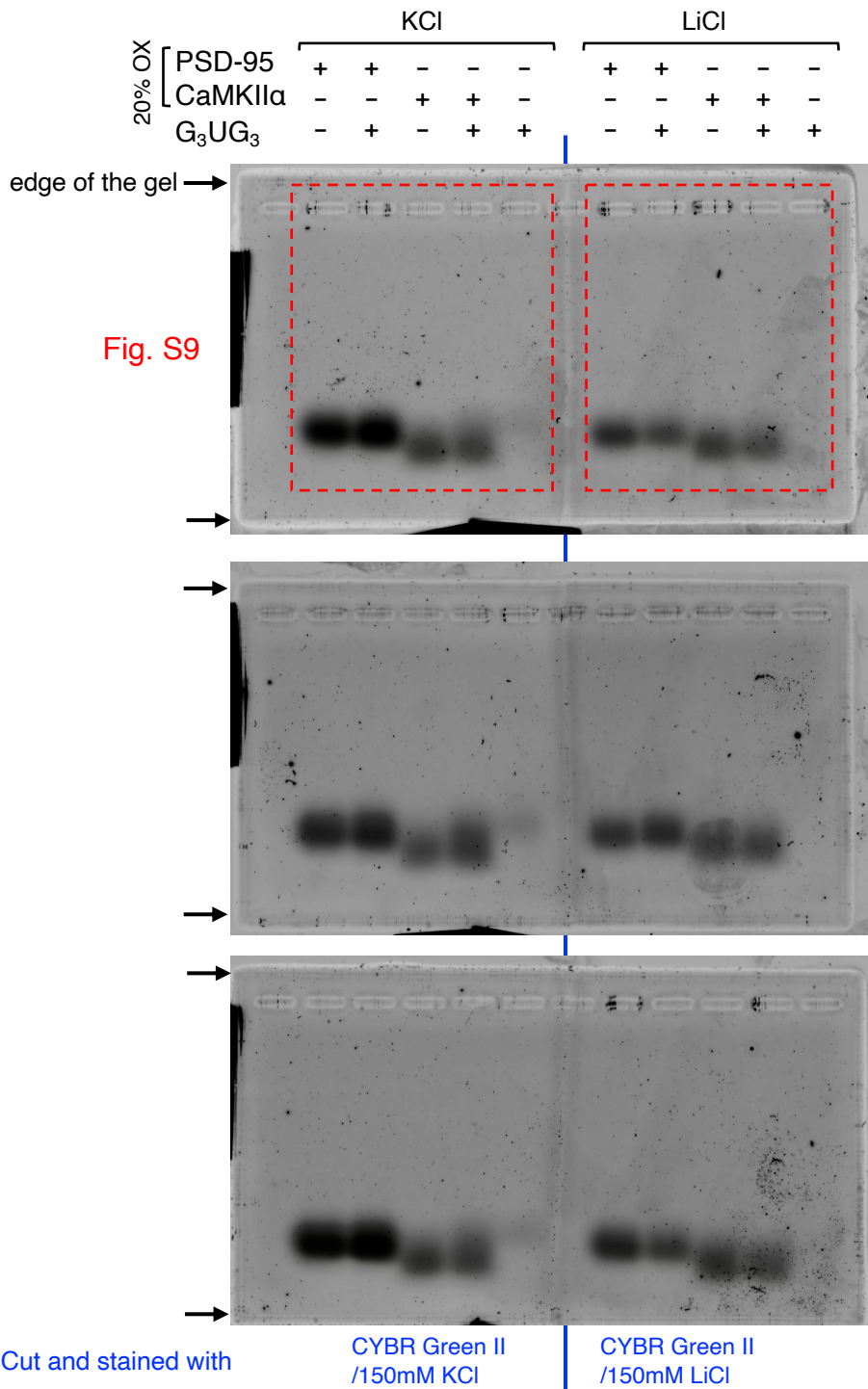


**Figure S10.** Original images of the gel shift assay (related to Fig. S9). The areas enclosed by the red dashed lines are used for Fig. S9. The samples containing potassium or lithium were electrophoresed simultaneously on the same gel, cut upon completion, and stained with a CYBR Green II staining solution containing 150 mM KCl or LiCl.

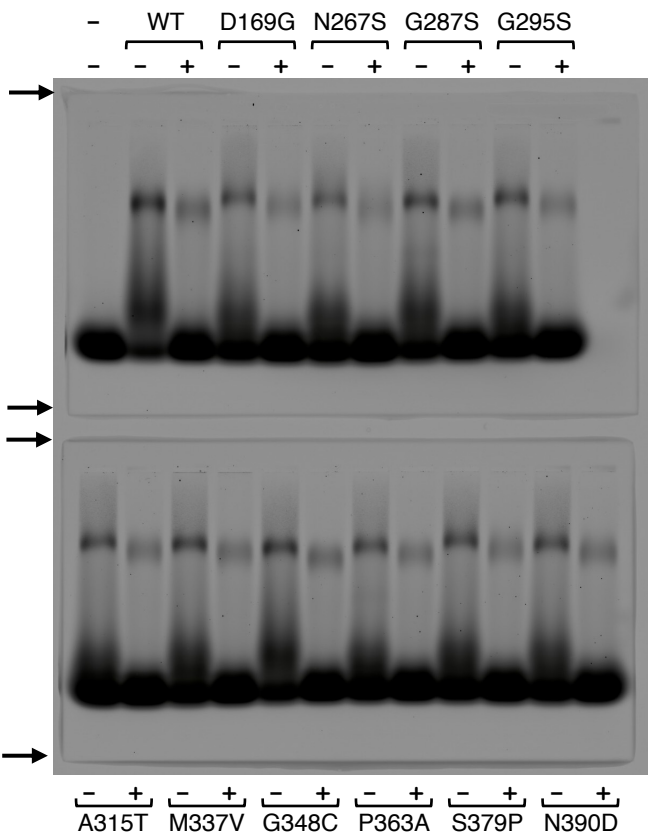
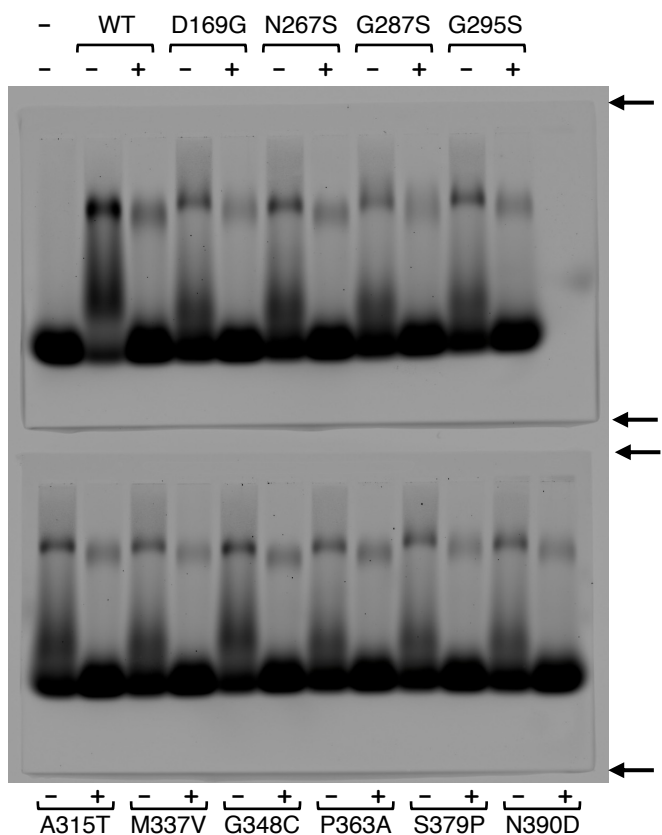
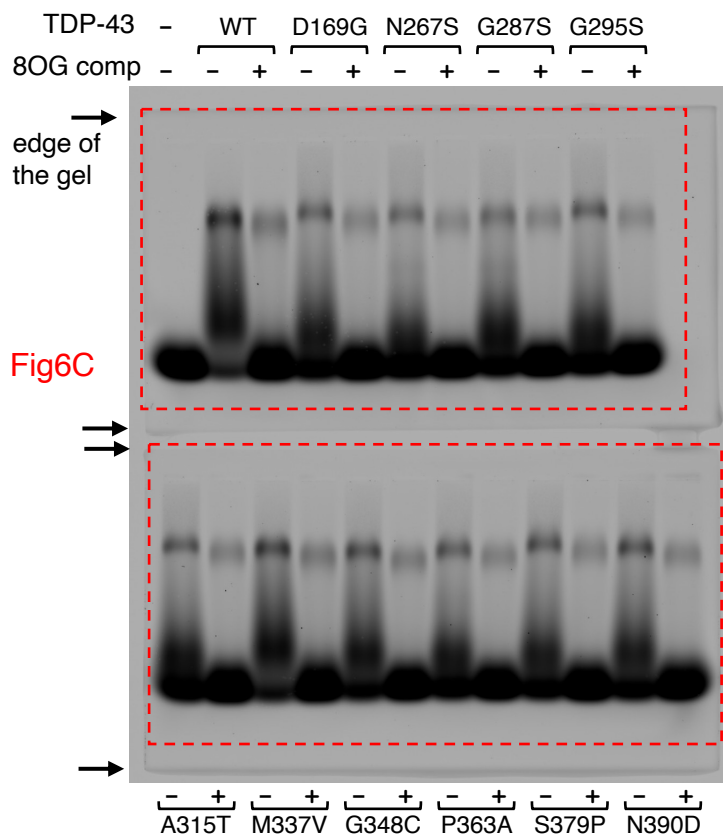


**Figure S11.** Original images of the gel shift assay (related to Fig. 6). The areas enclosed by the red dashed lines are used for Fig. 6C.